International Journal of
Computing and
Engineering
(IJCE)

Optimization of the Kawe DMA Water Network Using Genetic Algorithms: A Pathway to achieve UN SDG 6

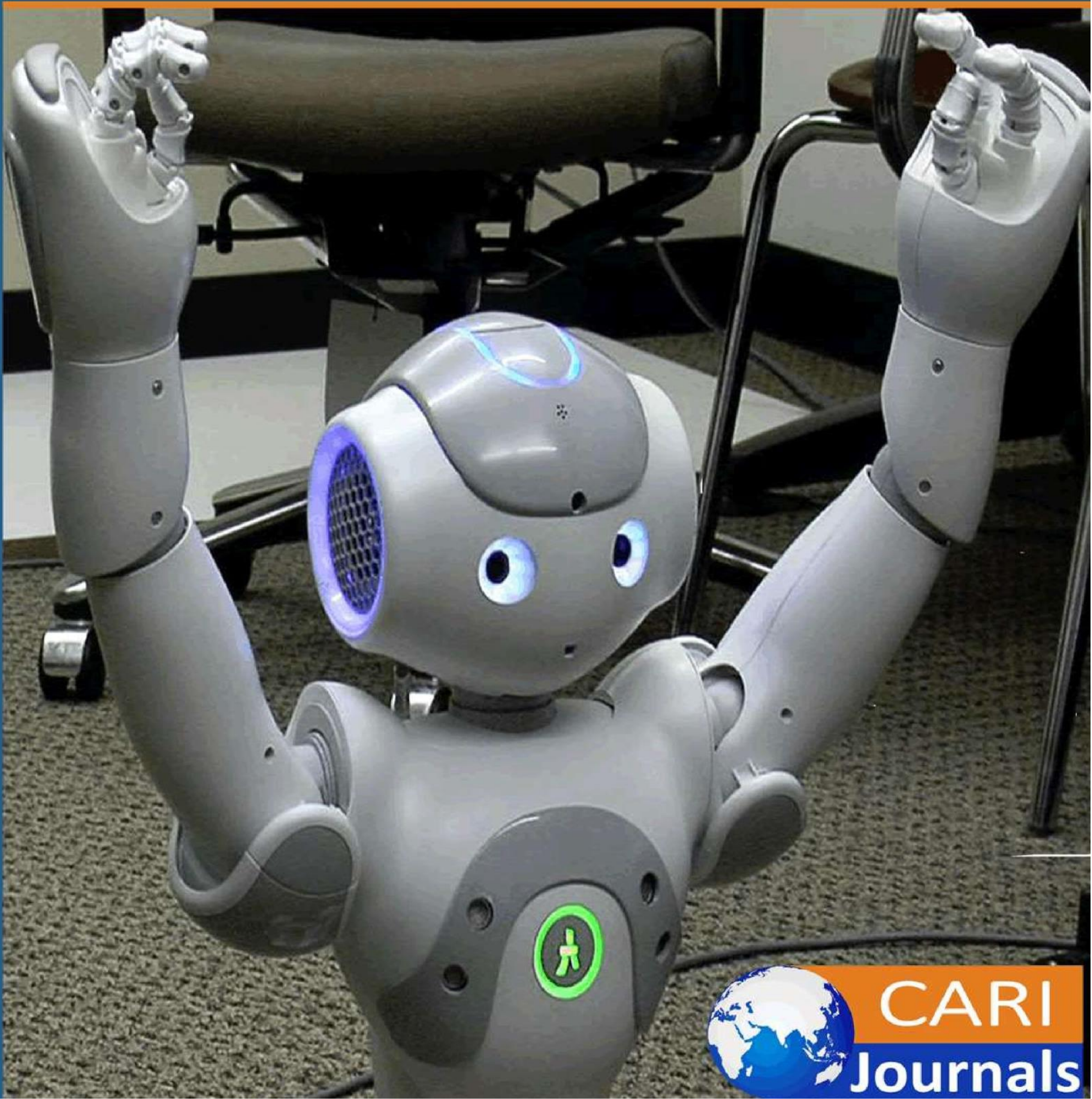

CARI Journals

International Journal of Computing and Engineering
ISSN 2958-7425 (online)
Vol. 7, Issue No. 21, pp. 12 - 31, 2025 www.carijournals.org

Optimization of the Kawe DMA Water Network Using Genetic Algorithms: A Pathway to achieve UN SDG 6

Lazaro Kisiri[1*], William Senkondo[2]

[1,2]Department of Water Supply and Sanitation Engineering, Water Institute, Dar es Salaam, Tanzania

[1]Dar es Salaam Water Supply and Sanitation Authority, Dar es Salaam, Tanzania

https://orcid.org/0009-0002-3536-0594

Crossref

Accepted: 29th June, 2025, Received in Revised Form:19th July, 2025, Published: 12th Aug, 2025

ABSTRACT

Purpose: This study aims to develop a cost-effective and pressure-resilient pipe replacement strategy for the Kawe District Metered Area (DMA) in Dar es Salaam, Tanzania, to improve hydraulic performance amid aging infrastructure and shifting demand in urban water networks.

Methodology: A Multi-Objective Genetic Algorithm (MOGA) was used to generate pipe layouts balancing investment cost and hydraulic performance. Optimization and EPANET-based pressure evaluations were executed in Python for integrated modeling and analysis. Alternatives were screened using multi-criteria evaluation based on reliability, cost-efficiency and feasibility. Sensitivity analysis tested robustness under 10% demand growth and 30% cost escalation.

Findings: The process yielded 38 Pareto-optimal layouts with nine selected for detailed review. All selected designs maintained minimum pressures above 5 m. The benchmark layout, involving two pipe replacements of total length of 0.409 km, achieved pressures of 9.87 m and 16.29 m at key junctions at a cost of TSh 19.08 million. Under sensitivity scenarios it sustained pressures above 8.66 m and 14.83 m without redesign.

Unique Contribution to Theory, Policy and Practice: This study contributes a scalable, pressure-aware planning framework integrating hydraulic modeling with evolutionary optimization. Theoretically, it advances multi-criteria decision-making in water infrastructure design. Practically, it equips utility planners with a data-driven tool for cost-efficient reinforcement of urban water networks. Policy-wise, it supports strategic investment planning aligned with Sustainable Development Goal 6, promoting equitable and resilient water service delivery.

Keywords: *Water Distribution System, Multi-objective Genetic Algorithm, Hydraulic Performance, Sensitivity Analysis, Sustainable Development Goal 6, Kawe DMA, Python*

JEL Codes: *C61, Q25, R58*

1.0 Introduction

In rapidly urbanizing cities such as Dar es Salaam, Tanzania, water distribution networks (WDNs) face mounting challenges due to aging infrastructure, fluctuating demand, and budget constraints. These issues often result in service inconsistencies, pressure losses, and unequal access to safe water particularly in underserved areas (World Bank, 2017; UN-Habitat, 2020). Addressing such challenges is central to Sustainable Development Goal (SDG) 6, and especially Target 6.1, which calls for "universal and equitable access to safe and affordable drinking water for all" (United Nations, 2015).

Hydraulic modeling has become a central tool for evaluating and planning interventions in WDNs. These models simulate pressure, flow, and demand dynamics across the network, offering decision-makers a diagnostic lens to assess service gaps, identify critical nodes, and evaluate the impact of infrastructure upgrades. Widely adopted platforms such as EPANET allow detailed analysis under varying system conditions, including fluctuating demands and temporal supply constraints (Rossman, 1993). Traditionally, utility engineers have relied on trial-and-error methods to improve network configurations by adjusting variables and re-running simulations until acceptable performance thresholds are met. This process becomes inefficient as the number of decision variables such as pipe replacement segments and selections from commercial pipe diameters continues to grow (Wu & Simpson, 2001).

To enhance planning, simulation–optimization frameworks integrate network modeling with computational algorithms to explore upgrade alternatives more efficiently (Mohan et al., 2007; Batista do Egito et al., 2023). Among these, Genetic Algorithms (GAs) are widely used for their flexibility in handling discrete, nonlinear problems (Goldberg, 1989; Savic & Walters, 1997), especially in scenarios involving pipe selection and budgetary trade-offs (Simpson et al., 1994; Dandy et al., 1996). Multi-objective GAs, in particular, generate Pareto-optimal designs that help planners balance cost and system performance (Farmani et al., 2005; Reca & Martínez, 2006). This study applies a MOGA-based optimization framework to the Kawe DMA in Dar es Salaam. Using hydraulic simulation and algorithm tuning, it identifies pipe replacement strategies that minimize cost while ensuring pressure and velocity compliance over a 24-hour cycle. The framework offers a replicable, data-driven approach to support practical utility planning and contribute to improved service delivery aligned with UN SDG 6.

2.0 Materials and Methods

2.1 Description of the Study Area

Kawe DMA is a subzone of the Kawe Distribution networks in northern Dar es Salaam, Tanzania's largest city, and operates under the Dar es Salaam Water and Sanitation Authority (DAWASA). Kawe DMA lies entirely within the Lower Ruvu Hydraulic Zone fed directly by the Lower Ruvu Water Treatment Plant (WTP)—and extends roughly from 6.72796° S, 39.217722° E in the northwest to 6.75031° S, 39.24355° E in the southeast. Elevations within the DMA range from

International Journal of Computing and Engineering
ISSN 2958-7425 (online)
Vol. 7, Issue No. 21, pp. 12 - 31, 2025 www.carijournals.org

about 4 m at the low-lying coastal fringe to nearly 39 m in the inland upland areas, imparting significant hydraulic head variation across the network.

Hydraulically, Kawe DMA is supplied through a single 54-inch trunk main equipped with an inline electromagnetic flow meter. The distribution network comprises 145 pipes totaling ~25 km in length, built from PVC (60%), steel (25%). Pipe diameters fall into three classes: 45–81 mm (70 pipes), 82–102 mm (29 pipes), and 103–203 mm (46 pipes). The intended service level for the DMA is continuous 24-hour supply. However, pressure issues remain, especially in central zones

The Kawe DMAs serves a diverse customer base, including 24 Commercial connections, 2384 Domestic connections, 1 Industrial connection, and 237 Institutional connections, totaling 2649 customers. The intended level of service in the DMA is 24-hours continuous supply, though operational challenges persist. Flow-meter data collected over seven days (January- April 2025) indicate an overall average hourly inflow of 35.82 L/s and an average daily peak of 36.88 L/s yielding a peak factor of 1.05 (for data of 17-23 February 2025). Figure 1 shows the geographic extent of Kawe DMA within Dar es Salaam and its principal hydraulic features.

International Journal of Computing and Engineering
ISSN 2958-7425 (online)
Vol. 7, Issue No. 21, pp. 12 - 31, 2025
www.carijournals.org

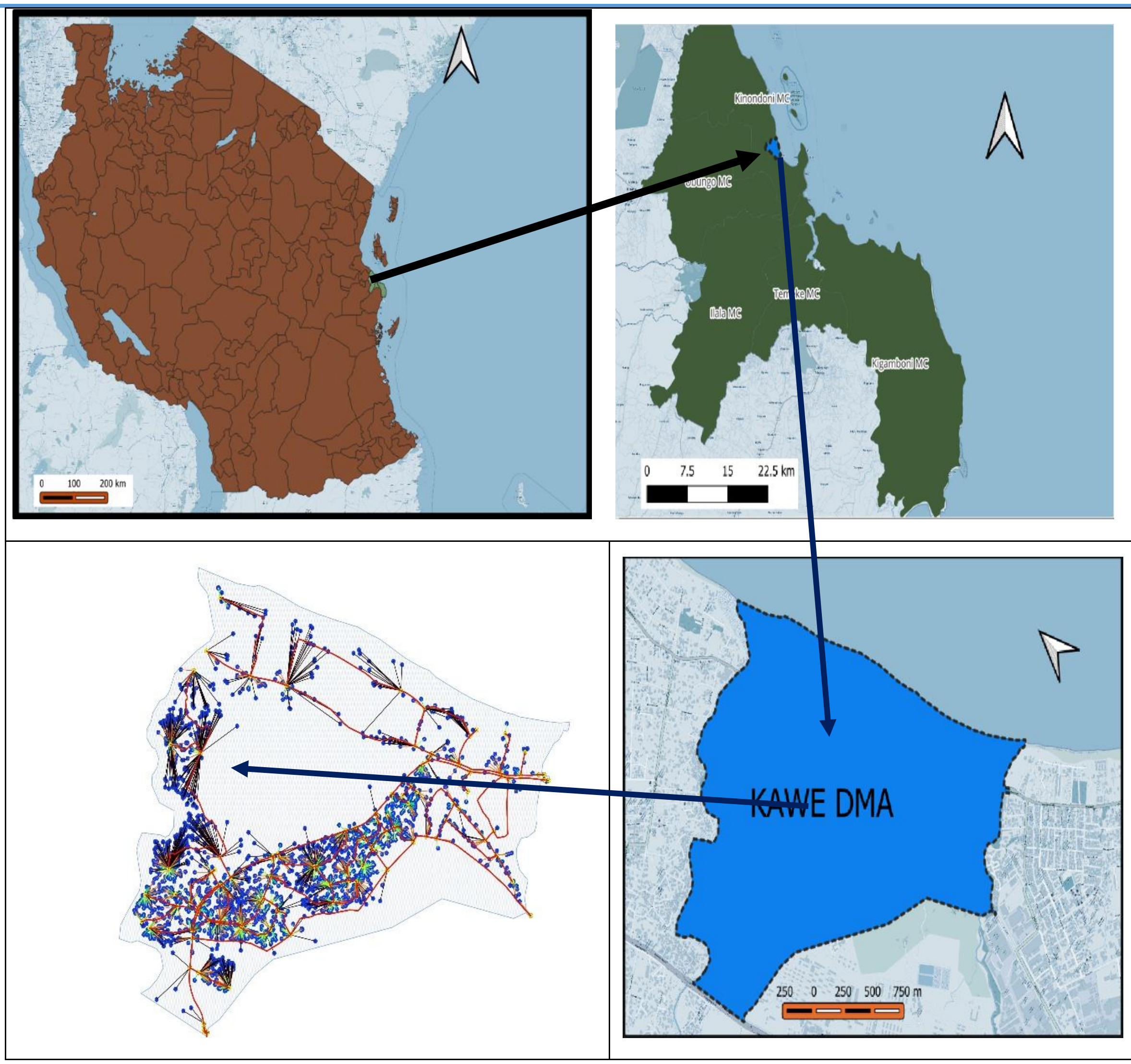

Figure 1: Map of Tanzania, Dar es Salaam showing Kawe District Metered Areas boundary and its water Distributing networks including Spatial customer location.

2.2 Data Preparation and Hydraulic Model Calibration

Data obtained from DAWASA included the water distribution map, global hydraulic model, georeferenced customer records (July 2024–March 2025), 15-minute inlet flow and pressure data, and recent pipe and valve upgrade logs. Customer billing, survey, and registry records were cleaned and integrated in QGIS to build a unified DMA geodatabase. GIS layers pipes, valves, pumps, and boundaries were extracted and topologically validated. Baseline, NRW, and average demands (July 2024–February 2025) were allocated to nearby pipes and junctions. The EPANET hydraulic model was calibrated using field data to ensure realistic pre-optimization behavior.

2.3 Simulation–Optimization of Water Supply Network.

This study employed a simulation–optimization framework designed to minimize total pipe replacement costs while ensuring hydraulic performance within regulatory bounds over a 24-hour extended period. A Multi-Objective Genetic Algorithm (MOGA) was deployed in Python, interfacing with the EPANET 2.2 hydraulic engine through PyEPANET. Chromosomes encoded commercial pipe diameter configurations for segments identified for replacement. Hourly hydraulic simulations were carried out across the extended-period horizon to evaluate nodal pressures and pipe velocities against acceptable limits of 5.0–50.0 m and 0.3–2.0 m/s, respectively.

The GA approach aligns with prior applications in water infrastructure optimization, notably the GANET model introduced by Savic and Walters (1997), which leveraged evolutionary algorithms for pipe network design. This was further enhanced by Vairavamoorthy and Ali (2000), who addressed pipe sizing under operational constraints. Chromosome evaluation was guided by hourly hydraulic outputs, with pressure and velocity compared against thresholds using penalty structures originally proposed by Wu and Simpson (2001). These dynamic penalty mechanisms were adopted following the methodology of Sangroula et al. (2022), who demonstrated that adaptive scaling facilitates improved convergence and robustness in pressure-sensitive networks. A composite objective function was formulated to guide the optimization. It minimized a combination of pipe replacement costs and time-varying penalty terms associated with constraint violations. Penalty coefficients were defined using a structured scaling approach, wherein pressures below 5.0 m were penalized using $\alpha_p = 10^9$, pressures above 50.0 m with $\alpha_p = 10^6$, and all velocity violations with $\alpha_v = 5 \times 10^7$. The full objective function and penalty terms are defined in equation 1.

$$\text{Min } f(D) = \sum_{i=1}^{n} ci(Di, Li) + \sum_{t=0}^{24}\left(\sum_{k=1}^{k} \boldsymbol{\Psi} j,t + \sum_{k=1}^{k} \boldsymbol{\phi} k,t\right) \ldots\ldots\ldots\ldots\ldots \text{ Equation 1}$$

The pressure penalty function $\Psi_{(j,\, t)}$ were defined using scaling coefficient as in Equation 2

$$\boldsymbol{\Psi}_{(j,\, t)} = \left\{ \begin{array}{ll} 10^9 \times (5 - P_{j,t})^2, & \text{if } P_{j,t} < 5 \\ 10^6 \times (P_{j,t} - 50)^2, & \text{if } P_{j,t} > 60 \\ 0, & \text{otherwise} \end{array} \right\} \ldots\ldots\ldots\ldots\ldots\ldots\text{Equation 2}$$

The corresponding velocity penalty function $\boldsymbol{\Phi}_{(k,\, t)}$ were defined as provided in Equations 3

$$\boldsymbol{\Phi}_{(k,t)} = \left\{ \begin{array}{ll} 5\times10^7 \times (0.3 - V_{k,t})^2, & \text{if } V_{k,t} < 0.3 \\ 5\times10^7 \times (V_{k,t} - 2.0)^2, & \text{if } V_{k,t} > 2.0 \\ 0, & \text{otherwise} \end{array} \right\} \ldots\ldots\ldots\ldots\ldots \text{ Equation 3}$$

International Journal of Computing and Engineering
ISSN 2958-7425 (online)
Vol. 7, Issue No. 21, pp. 12 - 31, 2025
www.carijournals.org

In this formulation, D= {D1, D2... Dn} denotes the set of decision variables representing discrete commercial pipe diameters. C_i (D_i, L_i) is the replacement cost per meter of pipe i, based on diameter Di and length Li. $\Phi_{(k,\ t)}$ and $\Psi_{(j,\ t)}$ are applied penalty for pressure penalty $^{j,t}_{p}$ and velocity penalty $^{k,t}_{v}$ at junction *j* and pipe *k* at time step *t*, respectively.

2.4 Evolutionary Configuration and Sensitivity Analysis

To balance cost minimization and hydraulic reliability in the Kawe DMA, the Multi-Objective Genetic Algorithm (MOGA) employed a Pareto-based selection mechanism utilizing fast non-dominated sorting. This approach maintained population diversity across competing hydraulic and financial objectives. An adaptive mutation operator was incorporated to preserve exploratory momentum: mutation intensity was incremented by 0.2 upon detection of stagnation in objective improvements over successive generations. Network design options were constrained to five commercially available pipe diameters, selected based on local procurement standards. These were referenced via a predefined cost lookup table, as shown in Table 1.

Table 1. Commercial Pipe Diameters and Unit Costs

S/N	Diameter (mm)	Unit Cost (TSh/m)
1	81.4	15,000
2	101.6	25,000
3	147.6	30,000
4	152.4	40,000
5	203.2	50,000

To assess the impact of algorithmic parameters on optimization outcomes, eight configurations of MOGA were executed. Each scenario was run over 150 generations, with specific variations in population size, mutation rate, and crossover probability detailed in Table 2.

Table 2. Multi-Objective Genetic Algorithm Optimization Scenarios

Scenario	Population	Mutation Rate	Crossover Rate
1	150	0.10	0.80
2	150	0.10	0.85
3	150	0.15	0.80
4	150	0.15	0.85
5	200	0.10	0.80
6	200	0.10	0.85
7	200	0.15	0.80
8	200	0.15	0.85

Sensitivity analysis was conducted to assess the adaptability and effectiveness of each configuration. Performance metrics included total replacement cost, penalty magnitude, and compliance with hydraulic constraints, Pareto front diversity, and fitness convergence trends. Additionally, constraint clearance timing and mutation impact dynamics were monitored throughout the simulation horizon. The adopted MOGA framework, inspired by evolutionary principles and supported by literature on Pareto-based selection (Sangroula et al., 2022), was intended to efficiently explore trade-offs between cost efficiency and service reliability in complex water distribution planning tasks for this DMA.

2.5 Post-Optimization Evaluation and Hydraulic Sensitivity Analysis

Post-optimization hydraulic assessments were conducted on selected network layouts using EPANET's Extended Period Simulation (EPS) across a full 24-hour demand cycle. Key performance metrics included average and minimum nodal pressures, pressure distribution range, and total penalty cost ensuring temporal stability under realistic demand conditions. Spatial behavior was evaluated via hourly pressure tracking at representative junctions to assess localized resilience and sensitivity. Design robustness was compared across normal and elevated demand scenarios, supporting identification of implementation-ready layouts. Pressure trends, penalty reductions, and cost efficiency were jointly reviewed to guide decisions on phasing and infrastructure upgrades.

2.6 Optimization and Genetic Algorithm Workflow

The optimization process for Kawe DMA integrated EPANET-based hydraulic simulation with a multi-objective Genetic Algorithm (GA). This approach aligns with established methodologies in water network optimization, as demonstrated by Deb et al. (2002) in evolutionary multi-objective frameworks and Farmani et al. (2005) in Pareto-based hydraulic design. More recent applications, such as Sangroula et al. (2022) and Kumar & Pramada (2023), have reinforced the effectiveness of simulation–optimization coupling for pressure-sensitive networks and cost-efficient planning. The complete workflow is illustrated in Figure 2, which summarizes the sequence from model setup to final layout validation.

International Journal of Computing and Engineering
ISSN 2958-7425 (online)
Vol. 7, Issue No. 21, pp. 12 - 31, 2025
www.carijournals.org

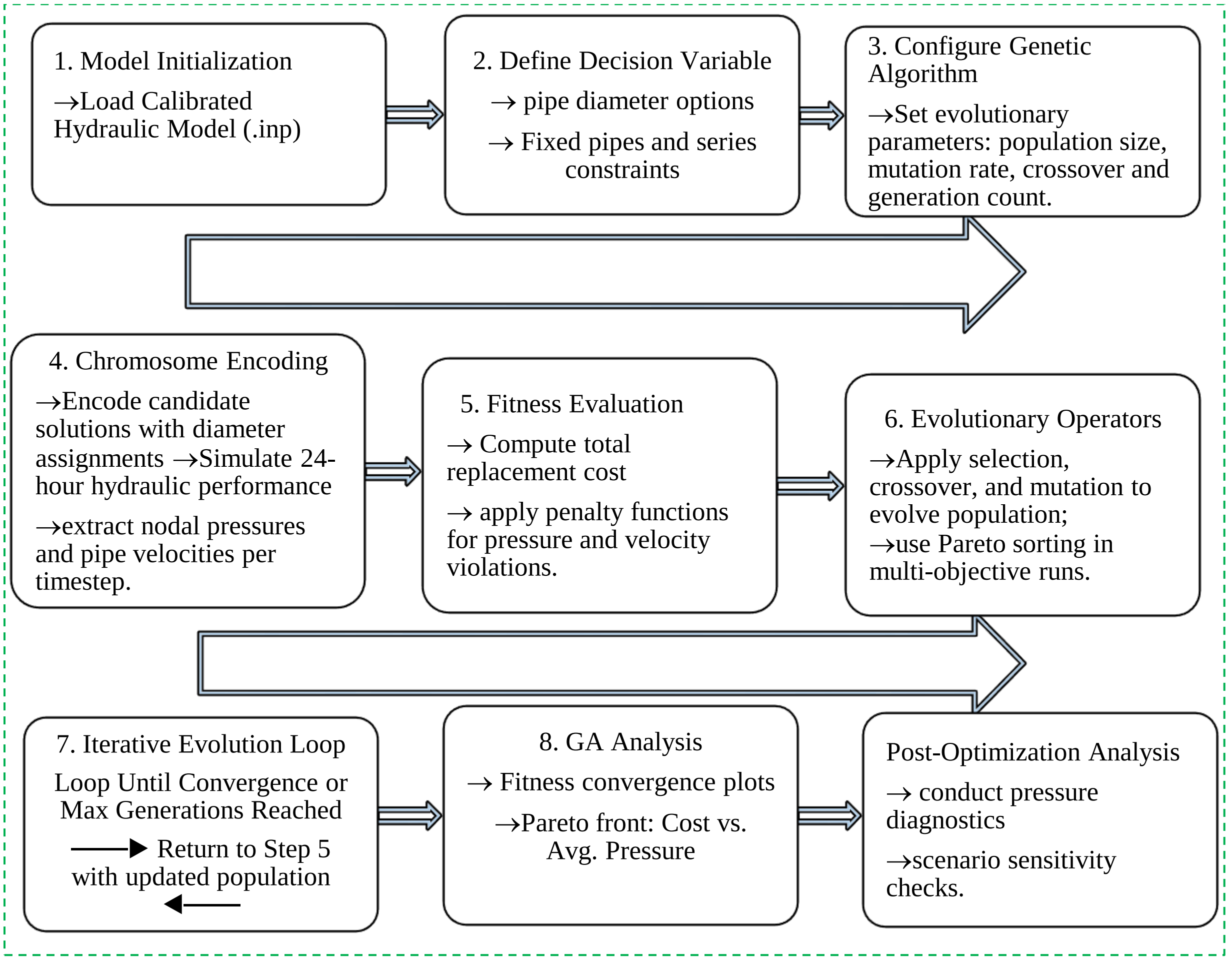

Figure 2: Modular optimization workflow integrating EPANET hydraulic simulation with multi-objective Genetic Algorithm.

3.0 RESULT AND DISCUSSION

3.1 Convergence Behavior and Performance Analysis

Convergence analysis across all eight GA configurations revealed a consistent two-phase trajectory—rapid early reduction in replacement cost followed by stabilization or divergence, depending on operator dynamics. Most scenarios achieved the elite solution of TSh 19.08×10^6 by Generation 5, indicating strong early-stage targeting. As shown in Table 3, Scenarios 1–3 and 8 preserved elite layouts across more than 97% of generations, supported by low mutation rates (0.10–0.15) and moderate crossover probabilities (0.80–0.85). Scenario 5 combined early feasibility with over 60 elite reappearances, while Scenario 6 showed drift beyond Generation 51. Scenario 4 exhibited early instability due to excessive crossover without sufficient mutation control. These outcomes validate the conclusion that convergence stability improves under selective pressure, low mutation intensity, and strong elitism—consistent with observations by

International Journal of Computing and Engineering
ISSN 2958-7425 (online)
Vol. 7, Issue No. 21, pp. 12 - 31, 2025 www.carijournals.org

Hassanat et al. (2019) and Patil & Pawar (2015), who emphasized structural preservation in multi-objective GA design.

Table 3: Summary of GA Configurations and Performance Metrics

Scenario	Final Cost (TSh)	Elite Stability	Penalty Cleared	Stability
1	20.50×10^6	Gen 3–150 (98.7%)	Generation 3	Very High
2	20.50×10^6	Gen 3–150 (98.7%)	Generation 3	Very High
3	20.50×10^6	Gen 5–150 (97.3%)	Generation 5	Very High
4	20.50×10^6	Gen 4–30 (18.0%)	Generation 4	Moderate
5	19.08×10^6	Gen 5–50 (30.7%)	Generation 5	High
6	20.82×10^6	Gen 4–51 (32.0%)	Generation 4	Moderate
7	20.50×10^6	Gen 3–150 (98.7%)	Generation 3	Very High
8	19.08×10^6	Gen 4–150 (98.0%)	Generation 4	Very High

3.1.1 Total Cost Convergence Profile across Scenarios

Total cost trajectories across the eight GA configurations revealed varied convergence behavior driven by mutation rate, crossover probability, and population size. Scenarios using mutation = 0.10 namely Scenarios 1, 2, 5, and 6 exhibited the most reliable cost stabilization. Scenario 5 (Pop = 200, Cross = 0.8) achieved the target cost of TSh 1.6238×10^{11} by Generation 5, maintaining it across 145 of 150 generations (96.7%) with minimal rebound. Similarly, Scenario 6 stabilized by Generation 4 and retained cost for 95.3% of the run, with brief post-plateau deviation. Scenario 1 achieved convergence by Generation 3 and held feasibility across >80% of generations, despite temporary spikes near Generation 135. Scenario 2 retained elite performance in >85% of generations, though minor fluctuations were noted during mid-phase evolution.

Scenarios configured with mutation = 0.15 revealed more variability, especially under higher crossover rates. Scenario 3 reached feasibility early and sustained the optimal cost over most generations, though rebounds occurred between Generations 70–82, peaking near TSh 1.6258×10^{11}. Scenario 4, despite early convergence, showed weak retention after Generation 30, with repeated surges reaching TSh 1.4438×10^{11}, indicating structural instability due to high crossover and limited selection control. In contrast, Scenarios 7 and 8 (Pop = 200, Mut = 0.15) performed favorably under well-calibrated settings. Scenario 7 maintained cost feasibility in 94.0% of generations, with frequent elite reappearances despite intermittent volatility. Scenario 8 yielded the most stable outcome, attaining TSh 1.6238×10^{11} by Generation 4 and preserving it for 147 consecutive generations (98%) without penalty drift. These results underscore the convergence advantage of pairing moderate mutation with large population size and balanced crossover.

International Journal of Computing and Engineering
ISSN 2958-7425 (online)
Vol. 7, Issue No. 21, pp. 12 - 31, 2025 www.carijournals.org

As illustrated in Figure 3, Scenarios 1, 2, 5, 6, 7, and 8 exemplify strong generational stability and elite cost control, confirming the utility of calibrated GA parameters in WDN optimization. The trends align with insights from Hassanat et al. (2019) and Patil & Pawar (2015) on the role of mutation moderation and crossover design in sustaining elite retention. By contrast, underperforming configurations such as Scenario 4 lacked sufficient structural preservation, compromising long-term feasibility. These findings reinforce the methodological soundness of the selected design space for cost-efficient pressure-sensitive system planning.

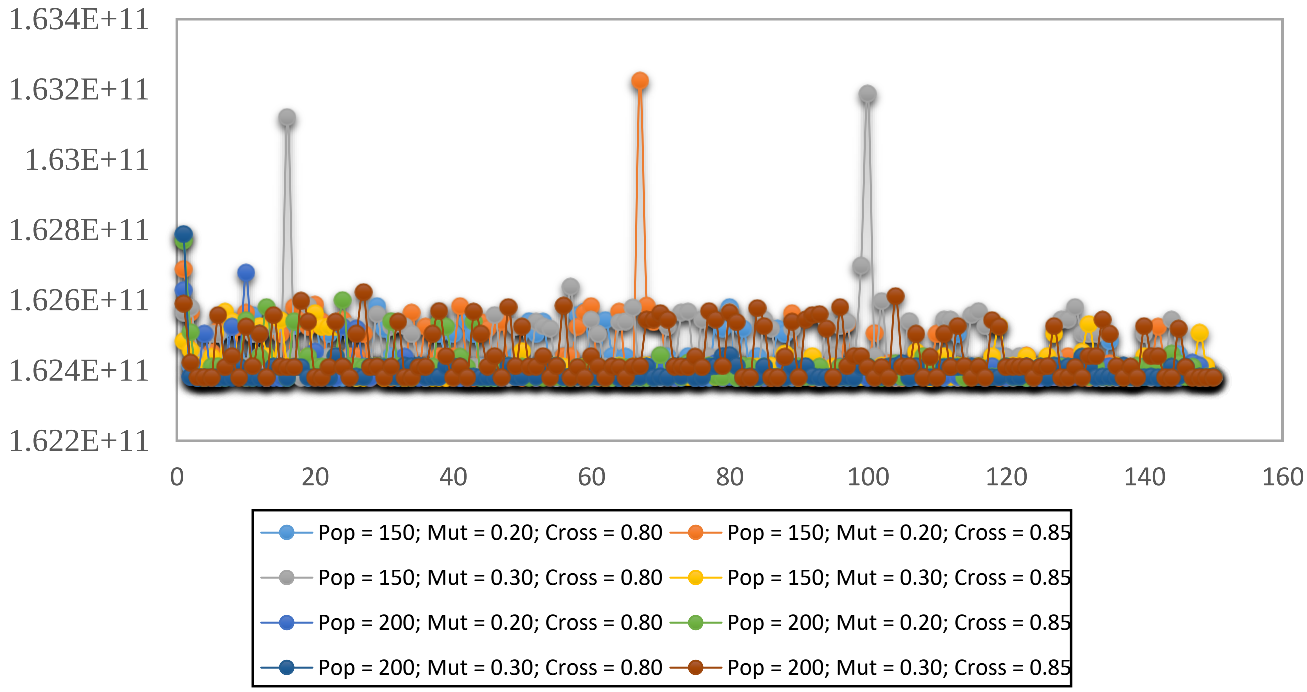

Figure 3: Total cost convergence across eight GA configurations for Kawe DMA optimization.

3.1.2 Replacement Cost Convergence Profile across Scenarios

Replacement cost convergence across the eight GA configurations demonstrated strong early-stage stabilization, with most scenarios reaching the optimal benchmark of TSh 19.08 × 10^6 within the first five generations. Scenario 8 (Pop = 200, Mut = 0.15, Cross = 0.85) delivered the highest level of structural retention—achieving the elite replacement cost by Generation 4 and maintaining it across 147 out of 150 generations (98%). No observable perturbations occurred throughout the simulation, confirming exceptional convergence stability. Likewise, Scenario 5 (Pop = 200, Mut = 0.10, Cross = 0.80) attained TSh 19.08 × 10^6 by Generation 5 and preserved this value through 34 uninterrupted generations, with repeated elite recoveries totaling 63 generations, despite transient spikes between Generations 94–107.

Scenario 6 demonstrated a stable plateau from Generation 4 to 51, followed by moderate variation and a final cost of TSh 20.82 × 10^6. Early convergence was also observed in Scenarios 1, 2, and 3,

International Journal of Computing and Engineering
ISSN 2958-7425 (online)
Vol. 7, Issue No. 21, pp. 12 - 31, 2025 www.carijournals.org

which each reached elite cost by Generation 3–5. Notably, Scenario 1 retained stability for >80% of the run, while Scenario 2 held until Generation 80 with intermittent rebounds. Scenario 3 maintained the target value until Generation 69, then showed short-lived deviations. Scenario 4, however, diverged post-Generation 30, peaking at TSh 23.02×10^6 with reduced layout retention.

The comparative behaviors of Scenarios 7 and 8, both configured with mutation = 0.15 and population = 200, illustrate the nuanced interplay between diversity and structural control. Scenario 7 achieved elite cost by Generation 3, held it for ~22 generations, and recorded ~18 elite recoveries afterward, despite replacement cost surges up to TSh 23.02×10^6 at Generation 42. Scenario 8, by contrast, sustained elite convergence uninterrupted, achieving the most stable trajectory among all configurations. These patterns reinforce convergence models proposed by Hassanat et al. (2019) and Patil & Pawar (2015), highlighting how tuning mutation and crossover rates enhances elite preservation and suppresses structural volatility in pressure-sensitive WDN optimization.

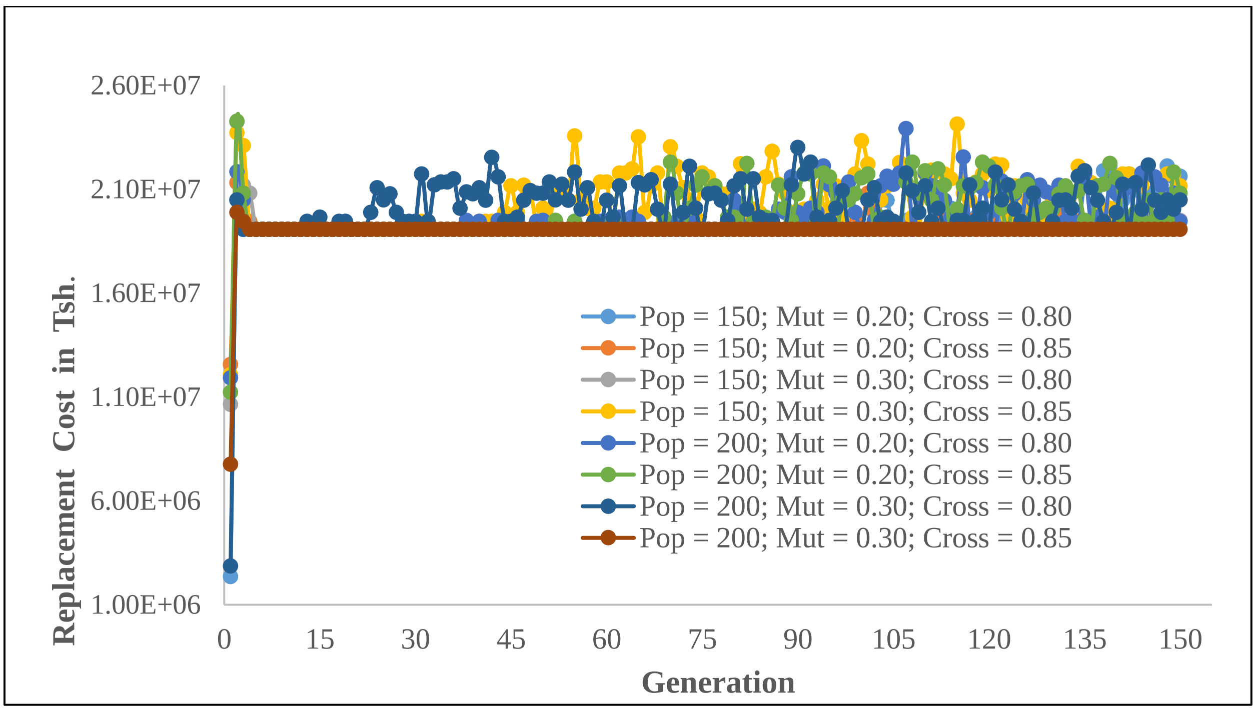

Figure 4: Replacement cost convergence behavior across eight GA scenarios.

3.2 Trade-Off Analysis between Optimized Cost and Hydraulic Penalty

To assess the investment–reliability trade-off in Kawe DMA, Pareto fronts were extracted from the final generation of each GA scenario based on NSGA-II principles (Deb et al., 2002). Table 2 summarizes 38 hydraulically feasible, non-dominated pipe layouts identified across eight configurations. Lower mutation scenarios (1, 2, and 5) exhibited denser trade-offs, stable convergence, and well-distributed fronts. Scenario 5 yielded eight cost-efficient layouts with wide

International Journal of Computing and Engineering
ISSN 2958-7425 (online)
Vol. 7, Issue No. 21, pp. 12 - 31, 2025 www.carijournals.org

variation; Scenario 2 produced designs from TSh 20.5M to TSh 36.6M. Scenario 1 provided five moderate options with compact diversity. By contrast, higher mutation settings (4, 7, and 8) led to narrow fronts with limited variation. Scenario 8 had the lowest-cost layout (TSh 19.08M) but just two solutions.

The solution space spans both performance-optimized and budget-sensitive layouts, enabling flexible reinforcement planning. Broad fronts like Scenario 5 reveal strong exploratory potential, supported by larger populations and well-tuned operators. Narrow yet feasible fronts in Scenarios 3 and 7 reflect controlled convergence with minimal structural overhead. These patterns reaffirm findings from Farmani et al. (2005) and Reed et al. (2013), emphasizing how mutation intensity and elite retention shape diversity and trade-off geometry. GA configurations with mutation rates of 0.10–0.15 and crossover values of 0.80–0.85 consistently yielded hydraulically compliant, cost-aware layouts. Table 4 summarizes these characteristics, providing planners with adaptable, investment-conscious options aligned with system constraints.

Table 4: Pareto Front Characteristics across Genetic Algorithm Scenarios

Scenario	Pop–Mut–Cross	Pareto Solutions	Cost Range (TSh)	Observation
1	150–0.15–0.8	6	20.5M–36.6M	Broad but structurally strong
2	150–0.15–0.85	5	19.5M–27.6M	Compact and low-cost front
3	150–0.2–0.8	4	21.1M–30.6M	Sparse, influenced by mutation
4	150–0.2–0.85	8	19.5M–43.7M	Wide diversity, highest spread
5	200–0.15–0.8	5	20.8M–29.4M	Balanced cost–penalty zone
6	200–0.15–0.85	3	21.3M–24.0M	Narrow front, lower diversity
7	200–0.2–0.8	2	19.08M–22.2M	Lowest replacement cost
8	200–0.2–0.85	6	20.5M–36.6M	Broad but structurally strong

3.3 Post-Optimization Evaluation of Selected Design Alternatives

While the multi-objective optimization framework produced 38 Pareto-optimal configurations across eight GA scenarios, utility planning requires the adoption of reference designs that balance cost, hydraulic benefit, and feasibility. Accordingly, a curated subset of nine alternatives was selected for post-evaluation, comprising eight knee-point layouts representing strategic trade-offs and one minimal-cost baseline derived from Scenario 8.

3.3.1 Pressure–Cost Trade-Offs

Performance comparisons across the nine optimized design alternatives revealed clear trade-offs between replacement cost, pressure reliability, and penalty resolution. As shown in Figure 4, all configurations surpassed the minimum pressure threshold of 10 m, ensuring continuous service across the Kawe DMA. The highest-performing layouts in terms of pressure outputs were

Alternative 1 and Alternative 2, with average pressures of 21.224 m and 21.225 m, and minimum pressures of 9.790 m and 9.780 m, respectively. These alternatives also incurred the highest penalty costs, exceeding TSh 162.4 billion, indicating significant constraint intensity despite strong hydraulic stability. Alternative 3, with an investment cost of TSh 20.88 million, achieved an average pressure of 21.170 m and a minimum of 9.770 m, reflecting good reliability at a mid-range budget.

Alternatives 4, 5, and 6 maintained pressure levels between 21.177 m and 21.219 m, with minimum pressures of 9.770–9.780 m and costs between TSh 22.68 million and 24.37 million. These layouts showed stable performance profiles under moderate cost inputs. Alternative 7 and Alternative 8, at roughly TSh 21.31 million and TSh 22.24 million, respectively, returned average pressures around 21.172–21.171 m and minimum values of 9.770 m, maintaining pressure compliance with modest variation. Most notably, Alternative 9 achieved full feasibility with the lowest cost TSh 19.08 million, 21.167 m average pressure, and a penalty of TSh 162.39 billion. It presents a cost-effective option suitable for phased upgrades.

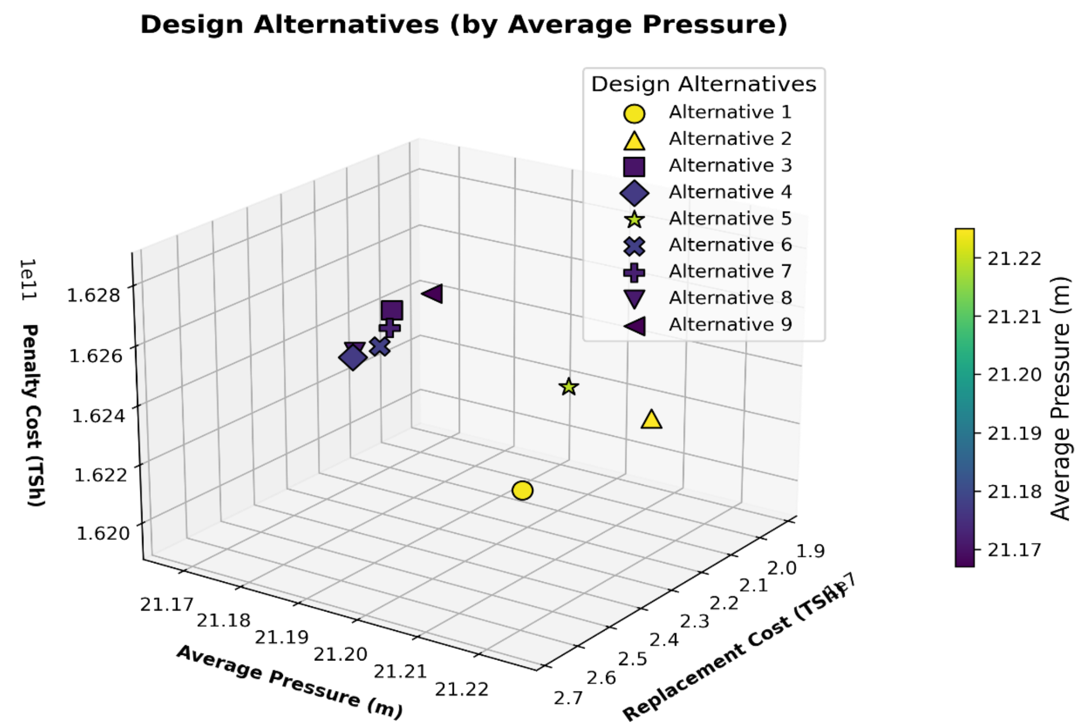

International Journal of Computing and Engineering
ISSN 2958-7425 (online)
Vol. 7, Issue No. 21, pp. 12 - 31, 2025
www.carijournals.org

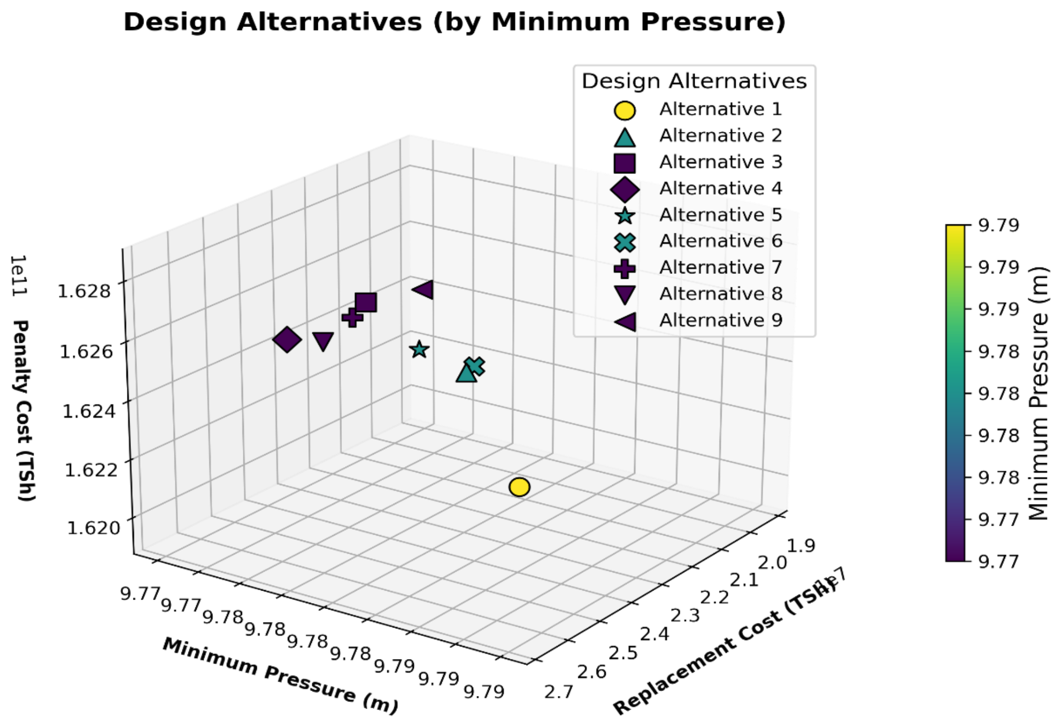

Figure 4: Relationship between pressure, replacement cost, and constraint penalty for all nine optimized alternatives.

3.3.2 water supply System Pressure Behavior over Time

Over the 24-hour EPS cycle, pressure patterns across the nine optimized layouts demonstrated strong and consistent hydraulic performance. The lowest recorded junction pressure was 9.770 m, observed in Alternatives 3, 4, 7, 8, and 9, while Alternative 1 maintained the highest minimum pressure of 9.790 m, affirming full compliance with the 10 m service threshold. When examining average minimum nodal pressures, Alternative 1 again led at 11.253 m, followed by Alternative 2 (11.244 m), with the lowest value—11.226 m—from the baseline layout (Alternative 9), which still surpassed operational requirements.

Average system pressures showed remarkable convergence across all alternatives, ranging narrowly between 21.167 m (Alternative 9) and 21.225 m (Alternative 2). Alternatives 1 and 2 delivered the most favorable averages (21.224–21.225 m), with Alternative 5 close behind at 21.219 m. Standard deviation values were clustered near zero across all junctions, indicating strong spatial uniformity. Only a few localized nodes exhibited slightly elevated variability, which is typical of demand-driven fluctuations and layout geometry. As shown in Figure 4, the full scatter of nodal pressures illustrates temporal and spatial stability, with most readings concentrated between 21–23 m. No layout exhibited pressure below 9.770 m at any point, confirming that all nine configurations deliver reliable service under daily demand conditions.

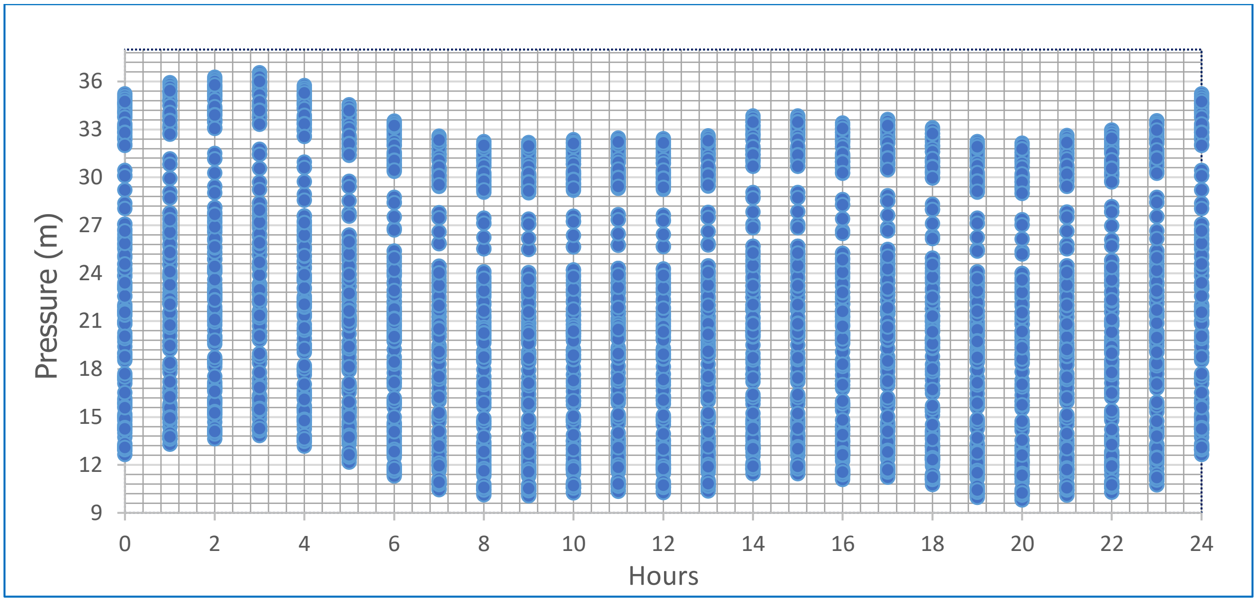

Figure 5: Scatter of all nodal pressures over time across the 24-hour EPS for all optimized layouts. Each point represents a junction's pressure at a given hour.

3.3.3 Pressure behavior at Critical Nodes under Baseline Conditions

To evaluate local pressure restoration under baseline conditions, pressure performance was assessed at two hydraulically significant nodes: Junction 356, located at the network periphery, and Junction 5410, positioned internally with previously suboptimal delivery. The baseline network recorded average pressures of 2.35 m and 8.77 m, with minimums dropping to 0.44 m and 6.76 m—well below acceptable service thresholds. These deficiencies reflected insufficient head during peak periods and broader system imbalance. Following optimization, all nine design alternatives restored compliant delivery. At Junction 356, average pressures rose to 11.35–11.46 m, and minimums to 9.87–9.97m indicating substantial recovery at the network's edge. Junction 5410 achieved averages between 17.77–17.85 m, with minimums from 16.29–16.36 m, confirming robust pressure stabilization internally. Table 5 illustrates the improvement in average pressure at both nodes across all optimized designs.

International Journal of Computing and Engineering
ISSN 2958-7425 (online)
Vol. 7, Issue No. 21, pp. 12 - 31, 2025 www.carijournals.org

Table 5: Pressure Performance at Junction 356 and Junction 5410 Before and After Optimization

Configuration	Junction	Avg. Pressure (m)	Min. Pressure (m)
Initial Baseline Network	Junction 356	2.35	0.44
	Junction 5410	8.77	6.76
Alternative 1	Junction 356	11.46	9.97
	Junction 5410	17.85	16.36
Alternative 2	Junction 356	11.43	9.95
	Junction 5410	17.84	16.35
Alternative 3	Junction 356	11.36	9.87
	Junction 5410	17.78	16.29
Alternative 4	Junction 356	11.38	9.89
	Junction 5410	17.79	16.30
Alternative 5	Junction 356	11.41	9.93
	Junction 5410	17.83	16.34
Alternative 6	Junction 356	11.40	9.91
	Junction 5410	17.79	16.30
Alternative 7	Junction 356	11.36	9.88
	Junction 5410	17.78	16.29
Alternative 8	Junction 356	11.37	9.88
	Junction 5410	17.78	16.29
Alternative 9	Junction 356	11.35	9.87
	Junction 5410	17.77	16.29

3.3.4 Sensitivity to Demand and Cost Variations

To assess the robustness of the optimized alternatives under uncertainty, two sensitivity scenarios were evaluated: a +10% increase in billed demand and a +30% rise in pipe unit costs. All nine layouts remained hydraulically compliant under elevated demand. Pressures at Junction 356 declined from 11.35–11.46 m to 8.66–8.79 m, but minimums pressure stayed above 7.14 m. Internally, Junction 5410 showed greater stability, with pressures decreasing from 17.77–17.85 m to 14.83–14.91 m and minimums remaining above 13.19 m.

These behaviors are visualized in Figure 6, comparing average pressure profiles under baseline and scaled demand. While Junction 356 exhibited higher sensitivity, both nodes retained safe pressure margins well above the 5 m threshold. In parallel, a 30% increase in unit costs raised capital estimates from TSh 24.8 million (Alt9) to TSh 34.7 million (Alt1) without affecting hydraulic layout or service delivery. This confirms that the optimized configurations are both technically stable and economically flexible under moderate uncertainty. These findings reinforce Page, P. R. (2006) affirming that pressure-optimized systems maintain viability amid demand and cost shifts. Overall, the results confirm that all nine solutions offer planners robust, adaptable, and pressure-compliant designs under variable conditions.

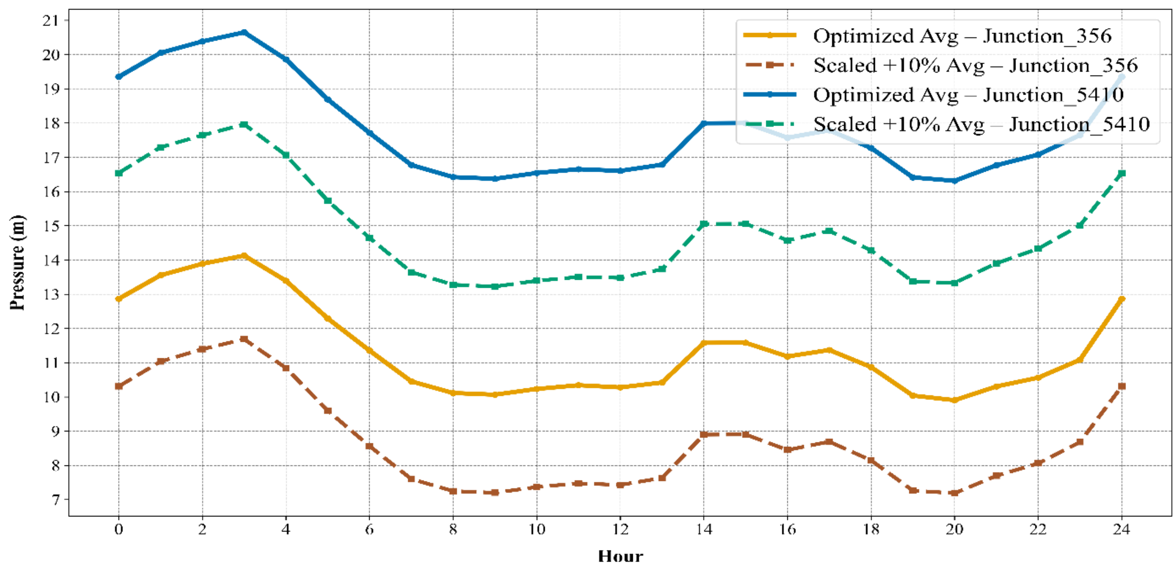

Figure 6: Average pressure response at Junction 356 and Junction 5410 under baseline and +10% demand conditions for all optimized alternatives.

3.3.5 Baseline Configuration as a Benchmark for Optimized Network Design

An optimization-based assessment produced 38 Pareto-optimal layouts for Kawe DMA. From these, nine were selected for post-evaluation based on hydraulic feasibility, structural diversity, and convergence traits. Two standout designs from Scenario 8 emerged one maximizing hydraulic enhancement, the other favoring cost efficiency. The first was the knee-point layout (alternative 8 as in Table 5) which achieved early convergence and sustained dominance across 150 generations. It involved four pipe replacements totaling 0.535 km, with a cost of TSh 22.24 million and a residual penalty of 1.6236×10^{11} TSh-equivalent. While hydraulically robust, its higher investment requirement made it less suitable for immediate implementation. The second and ultimately adopted baseline configuration (alternative 9 in Table 5) includes two targeted interventions totaling 0.409 km, with diameter enhancements from 147.6 mm to 203.2 mm and 76.6 mm to 81.4 mm as shown in Table 6. This layout achieved full hydraulic feasibility at the lowest recorded cost of TSh 19.08 million, while retaining the structural integrity and generational stability of its parent design. Its simplicity and cost-effectiveness make it the preferred benchmark for phased rehabilitation planning in Kawe DMA.

Comparable studies have demonstrated the effectiveness of multi-objective optimization approaches and parameter-sensitive algorithms in achieving balanced water network designs. Dandy et al. (1996)

and Savic & Walters (1997) demonstrated that genetic algorithms can yield reliable, budget-conscious designs. Zhu et al. (2023) achieved a 37.4–64.6% reduction in scattered pipe replacements using spatial clustering, and Kumar & Pramada (2023) confirmed that well-tuned genetic parameters enhance convergence and layout stability resulted in robust network designs. These findings align with the results in Kawe DMA, where the adopted baseline layout achieved full hydraulic feasibility at the lowest recorded cost. These results confirm that Kawe DMA can achieve reliable and spatially balanced service delivery through focused infrastructure interventions.

Table 6: specifications of baseline configuration

Configuration	Pipe ID	Existing Ø (mm)	Optimized Ø (mm)	Length (m)
Baseline (Alternative 9)	Pipe_1757	147.6	203.2	370.0
	Pipe_31	76.6	81.4	38.5

4. Conclusion and Recommendation.

This study provided 38 Pareto-optimal layouts through a multi-objective genetic algorithm to optimize pipe replacement strategies within the Kawe District Metered Area (DMA) in Dar es Salaam, Tanzania. Nine representative alternatives were selected for post-evaluation, all showing substantial hydraulic improvements under baseline conditions with pressures above 5 m. one design Alternative derived from Scenario 8, was selected as the final benchmark layout. It involved two targeted pipe replacements totaling 0.409 km and achieved minimum pressures of 9.87 m and 16.29 m at key junctions, with the lowest investment cost of TSh 19.08 million.

Sensitivity analysis confirmed that all nine layouts remained hydraulically compliant under elevated demand and cost scenarios. Under a 10% increase in billed demand, minimum pressures at Junction 356 and Junction 5410 remained above the 5 m threshold. For the alternative selected as benchmark pressures declined to 8.66 m and 14.83 m, maintaining resilience. A 30% rise in pipe unit costs increased its capital estimate to TSh 24.80 million, but no reconfiguration was required. These findings reflect strong adaptability and technical stability under uncertainty.

Based on these results, phased implementation of baseline alternative is recommended, starting with priority interventions to recover pressure cost-effectively. Hydraulic monitoring should be introduced post-rehabilitation, and the optimization methodology extended to other DMAs with similar constraints. Embracing algorithm-based planning will support strategic investments, enhance system resilience, and contribute to Sustainable Development Goal 6 by advancing equitable and reliable access to clean water.

Acknowledgments The author thanks Dr. William Senkondo and Dr. Livingstone Swilla for their guidance and support. Gratitude is also extended to DAWASA staff for their assistance with field data.

Data Availability The data supporting this study's findings are available from the author upon request.

Conflict of Interest The author declares no conflict of interest related to this study.

REFERENCES

Alperovits, E., & Shamir, U. (1977). Design of optimal water distribution systems. *Water Resources Research*, *13*(6), 885–900. https://doi.org/10.1029/WR013I006P00885

Batista do Egito, T., de Azevedo, J. R. G., & Bezerra, S. T. M. (2023). Optimization of the operation of water distribution systems with emphasis on the joint optimization of pumps and reservoirs. Water Supply, 23(3), 1094–1105.

Dandy, G. C., Simpson, A. R., & Murphy, L. J. (1996). An improved genetic algorithm for pipe network optimization. *Water Resources Research*, *32*(2), 449–458.

Deb, K., Pratap, A., Agarwal, S., & Meyarivan, T. (2002). A fast and elitist multi objective genetic algorithm: NSGA-II. *IEEE Transactions on Evolutionary Computation*, *6*(2), 182–197.

Farmani, R., Walters, G. A., & Savic, D. A. (2005). Trade-off between Total Cost and Reliability for Anytown Water Distribution Network. *Journal of Water Resources Planning and Management*, *131*(3), 161–171.

Goldberg, D. E., & Holland, J. H. (1988). Genetic Algorithms and Machine Learning. *Machine Learning*, *3*(2), 95–99. https://doi.org/10.1023/A:1022602019183

Hassanat, A., Almohammadi, K., Alkafaween, E., Abunawas, E., Hammouri, A., & Prasath, V. B. S. (2019). Choosing Mutation and Crossover Ratios for Genetic Algorithms—A Review with a New Dynamic Approach. *Information 2019, Vol. 10, Page 390*, *10*(12), 390.

Kuma, H., & Abate, M. (2021). Evaluation of hydraulic performance of water distribution system for sustainable management: A case of Tulu Bolo town, Ethiopia. Water Resources Management, 35(10), 3439–3454. https://doi.org/10.1007/s11269-021-03000-4

Kumar, V. H. S., & Pramada, S. K. (2023). Selection of Real-Coded Genetic Algorithm parameters in solving simulation–optimization problems for the design of water distribution networks. *Water Supply*, *23*(12), 5046–5061. https://doi.org/10.2166/WS.2023.301

Montesinos, P., Walski, T. M., & Trachtman, G. (1999). Genetic algorithms for water distribution network design: A review. Water Resources Update, 114, 40–49.

PAGE, P. R. (2006). Smart optimization and sensitivity analysis in water distribution systems. Council for Scientific and Industrial Research (CSIR), Pretoria, South Africa.

Reca, J., & Martínez, J. (2006). Genetic algorithms for the design of looped irrigation water distribution networks. Water Resources Research, 42(5), W05416.

Rossman, L. A. (1993). EPANET User's Manual. U.S. Environmental Protection Agency, Risk Reduction Engineering Laboratory.

Sangroula, U., Han, K.-H., Koo, K.-M., Gnawali, K., & Yum, K.-T. (2022). Optimization of water distribution networks using genetic algorithm based SOP–WDN program. Water, 14(6), 851. https://doi.org/10.3390/w14060851

Savic, D. A., & Walters, G. A. (1997). Genetic algorithms for least-cost design of water distribution networks. Journal of Water Resources Planning and Management, 123(2), 67–77.

Simpson, A. R., Dandy, G. C., & Murphy, L. J. (1994). Genetic algorithms for pipe optimization. Journal of Water Resources Planning and Management, 120(4), 423–443.

UN-Habitat. (2020). Water and sanitation. https://unhabitat.org/topic/water-and-sanitation

United Nations. (2015). transforming our world: The 2030 Agenda for Sustainable Development.

Vairavamoorthy, K., & Ali, M. (2000). Optimal design of water distribution systems using genetic algorithms. Computer-Aided Civil and Infrastructure Engineering, 15(5), 374–382.

World Bank. (2017). Water and sanitation program: End of year report, fiscal year 2017.

Wu, Z. Y., & Simpson, A. R. (2001). Competent genetic–evolutionary optimization of water distribution systems. Journal of Computing in Civil Engineering, 15(2), 89–101.

Zhu, X., Hou, B., & Wu, S. (2023). Water distribution pipe replacement optimization based on spatial clustering. AQUA - Water Infrastructure, Ecosystems and Society, 72(5), 762–780.